

Role of Magnetic Reconnection in Coronal Heating

Dr. Aradhna Sharma

Assistant Professor, Department of Physics, DBS PG College, Dehradun, Uttarakhand, India

ABSTRACT

The outermost atmosphere of the Sun, called the corona, is some 200 times hotter than the surface of the Sun. The main source of energy for heating the corona is believed to be the magnetic field which dominates the corona. Magnetic reconnection is probably the most important mechanism for releasing magnetic energy and may, therefore, be important for coronal heating or micro-flaring. The best observational examples of reconnection in the corona are thought to be X-ray bright points, which are small-scale brightenings seen randomly throughout the whole corona. Theoretical models can not only explain the key observations relating to bright points, but they can also explain the complex three-dimensional structures often seen in bright points. In these models magnetic neutral points play a significant role as the centres for reconnection both in two and three dimensions.

KEYWORDS: magnetic, reconnection, corona, heating, dimensional, neural, bright, dimensions

INTRODUCTION

There is still little consensus on what mechanism can be credited with supplying heat to the Sun's corona. Among the most frequently invoked candidates are dissipation of waves and magnetic reconnection. Both processes are known to occur, but their relative contributions to heating have yet to be definitively quantified observationally.[1,2]

There is extremely strong evidence that magnetic reconnection is occurring throughout the corona at some rate. The coronal field is connected to photospheric flux concentrations, which are, in all the best observations, surrounded by photosphere unconnected to the coronal field, if not entirely unmagnetized. These flux concentrations move about, apparently at random, under the influence of granular and super-granular flows. If the coronal field lines remained anchored to the same pair of foot points over days or weeks, the coronal magnetic field would appear extremely tangled and complex. The coronal field outlined in extreme ultraviolet (EUV) images shows little sign of such tangling—in fact, it appears smooth enough to have been 'combed'. While it is still possible that complex tangling occurs at length scales below our present resolution.

How to cite this paper: Dr. Aradhna Sharma "Role of Magnetic Reconnection in Coronal Heating" Published in International Journal of Trend in Scientific Research and Development (ijtsrd), ISSN: 2456-6470, Volume-6 | Issue-4, June 2022, pp.731-736, URL: www.ijtsrd.com/papers/ijtsrd50179.pdf



Copyright © 2022 by author(s) and International Journal of Trend in Scientific Research and Development Journal. This is an Open Access article distributed under the terms of the Creative Commons Attribution License (CC BY 4.0) (<http://creativecommons.org/licenses/by/4.0>)



This attempt must address the fact that topological change of field lines does not automatically generate heat. We present one case of flux emergence where we have measured the rate of coronal magnetic reconnection and the rate of energy dissipation in the corona. The ratio of these two, P/Φ , is a current comparable to the amount of current expected to flow along the boundary separating the emerged flux from the pre-existing flux overlying it. We can generalize this relation to the overall corona in quiet Sun or in active regions. Doing so yields estimates for the contribution to coronal heating from magnetic reconnection. These estimated rates are comparable to the amount required to maintain the corona at its observed temperature.

Footpoint motions occur over all length scales and presumably so should the tangling. There is little evidence for it on the largest scales, which appear increasingly well fitted by potential fields over time. This fact gives a clear indication that coronal field lines are constantly being reconnected: uprooted from one footpoint and reattached to another.[3,4]

According to Faraday's law, this additional flux must have arisen through an electric field

$$\Phi = - \oint_C \mathbf{E} \cdot d\mathbf{l},$$

along the perimeter C of the surface.

If the coronal field had remained entirely potential throughout the emergence, the reconnection would have produced no coronal heating at all—there would have been topological change in the absence of

heating. The rate of electromagnetic work on the plasma is

$$P = I\dot{\Phi},$$

where I is the current flowing along perimeter C . Without coronal current, there is no electromagnetic work, and therefore no heating from the topological change.[5,6]

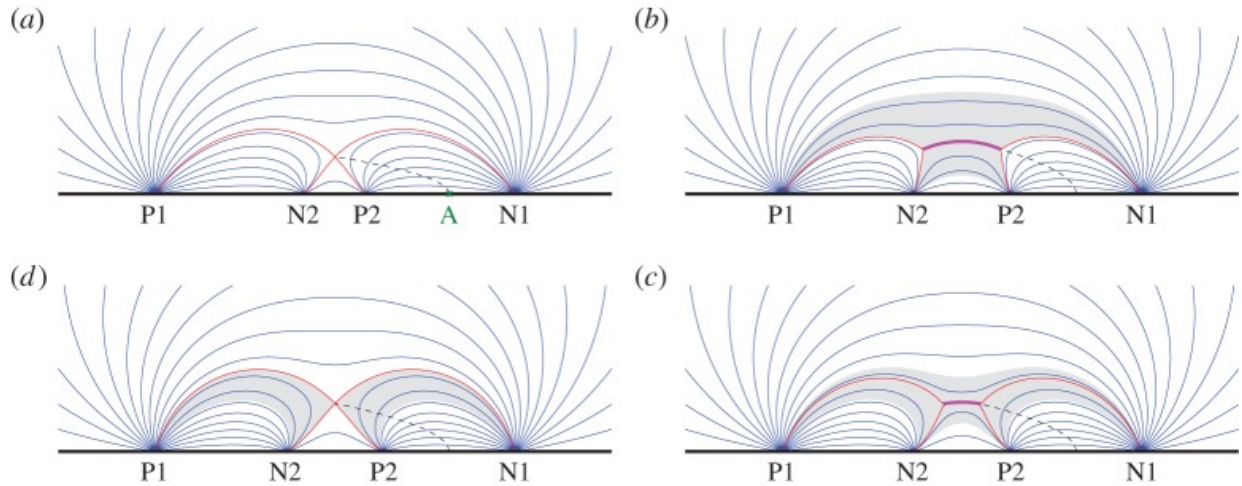


Figure 1: Stages, progressing clockwise from top left, in reconnection following the emergence of the bipole beneath an existing bipole. Field lines are blue curves originating in sources P1, P2, N1 and N2, located in the photospheric boundary (black horizontal line). (a) The pre-emergence state. (b–d) Stages after emergence of bipole P2–N2 have the same photospheric field: (b) the state before any reconnection, (c) after some reconnection and (d) the state after complete reconnection. Red lines show the separatrices, (thicker) magenta curves are the current sheet. The shaded region shows the flux that is reconnected to produce state (d) from state (b). Dashed curves show a surface through which flux connecting P2–N1 can be computed.

Heating occurs only when the magnetic reconnection is slow enough to permit the accumulation of current at the X-point. Figure 1b shows the case where no reconnection at all has occurred during the flux emergence. The flux interconnecting P2 and N1 is therefore the same as before emergence, and there is a current sheet separating the newly emerged from the pre-existing flux (The state with a current sheet is the one with the lowest magnetic energy subject to the single constraint on the interconnecting flux.) Any electric field within the current sheet will increase the P2–N1 flux, taking figure 1b to figure 1c. In this process, the magnetic energy will decrease by doing work on the plasma, endowing it with either heat or bulk kinetic energy. [7,8]

Discussion

Figure 2 shows 211 Å images² from AIA of the emerging bipole (a) along with radial field maps from HMI (b). The EUV images clearly show a dome of flux anchored in the newly emerged positive polarity, which we call P2 by analogy with figure 1. The newly emerged negative polarity has moved to the southeast, but the dome clearly includes negative polarity to the west: old flux, outlined in blue in figure 2b, and hereafter called N1. The distinction between old flux (N1) and new flux (N2) is made by tracking the evolution of the magnetograms, first automatically and then adjusting manually. This introduces the largest source of error into our calculation. One indication of its magnitude is that the total signed flux attributed to newly emerged flux remains constant within 10% of Ψ_2 over the primary emergence period—15 October.

The perimeter of the 211 Å dome was traced (manually) at 1 h intervals and mapped onto the HMI radial field maps (green curves). The total unsigned flux within this boundary remains constant to within 10% of Ψ_2 , suggesting that the boundary accurately identifies a closed magnetic system

The region of old negative flux (N1) lying within the dome perimeter was taken to be reconnected flux, analogous to the P2–N1 flux in figure 1. The integral of B_z over the overlapping region gives the reconnected $\Phi_r(t)$ shown as a red curve in figure 3. A crude linear fit to this (dashed line) rises at $\dot{\Phi}_r \simeq 2.9 \times 10^{15} \text{ Mx s}^{-1}$

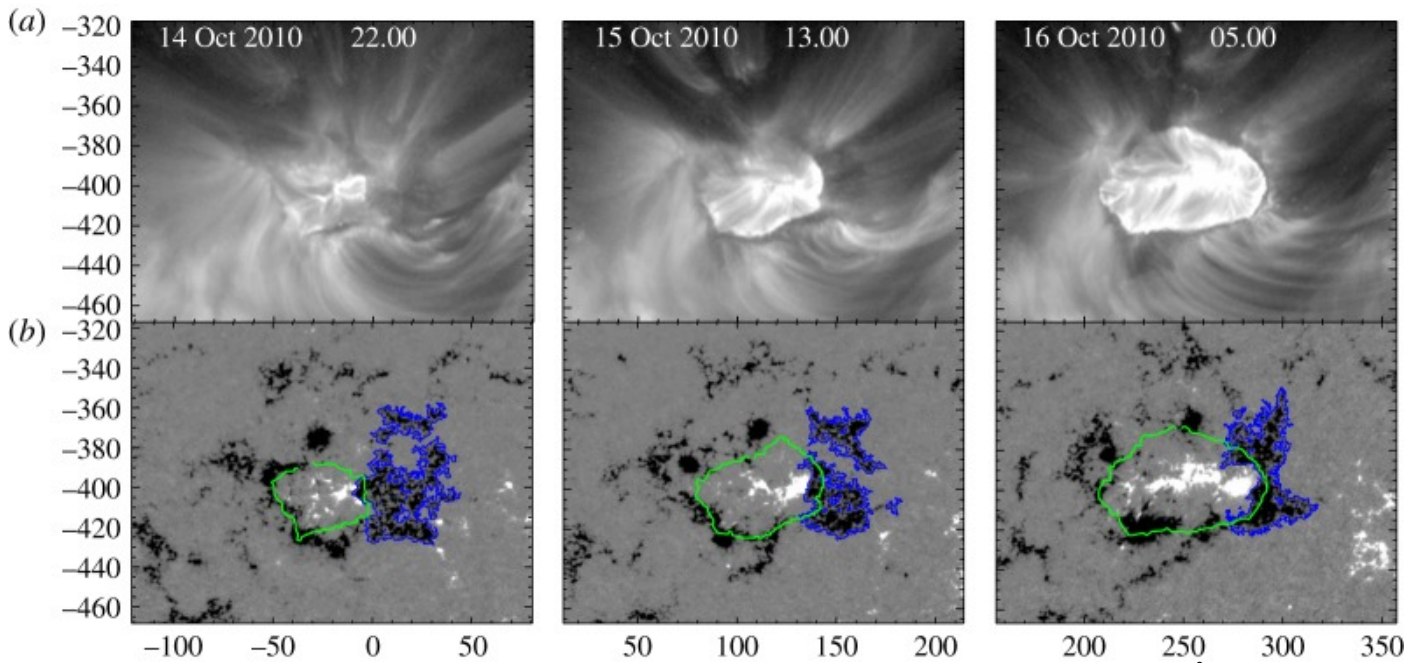


Figure 2: The emergence of a bipole into the negative polarity of AR 11112. (a) AIA 211 Å images from three times during the emergence, plotted with a logarithmic grey-scale. (b) HMI maps of $B_z(x,y)$ from the same times (on a grey-scale capped at ± 500 G). The green curves outline the dome from the 211 Å images, and the blue curves (to the right in each panel) outline the old negative polarity, N1, to which reconnection occurs.

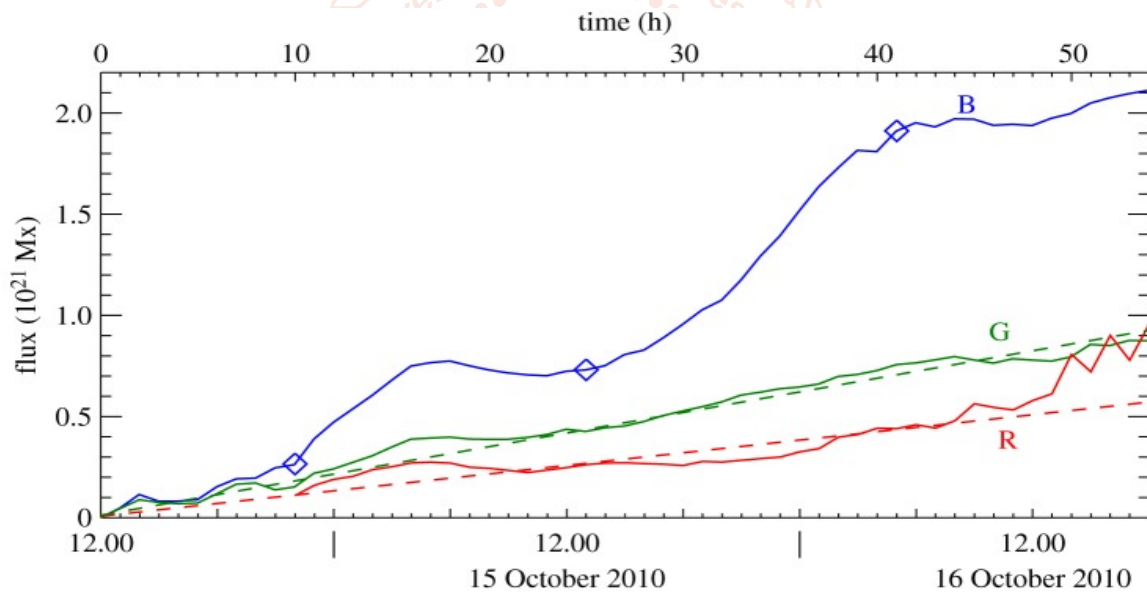


Figure 3: The fluxes from the emerging bipole over time. The blue curve (B) shows the total flux in the positive polarity P2 in units of 10^{21} Mx (maxwells). Diamonds mark the times of the panels in figure 2. The red curve (R) is $\Phi_r(t)$ found from integrating the portion of the old negative polarity within the dome. The green curve (G) is the amount of reconnected flux in a potential field, $\Phi_r^{(v)}(t)$. Dashed lines are linear fits, both intersecting zero at 11.15 on 14 October.

In a simplistic view of this process, the emerging flux reconnects to its surroundings in order to reduce its magnetic energy, and thereby approach a potential field. The reconnection is therefore driven by the difference in fluxes between the actual interconnecting flux and that in a potential field,

$$\Delta\Phi = \Phi_r^{(v)} - \Phi_r, \quad 3.1$$

which is the separation between the green and red curves in figure 3. This flux difference is plotted in violet in figure 4. In order to plot it with P_r , the flux difference $\Delta\Phi$ is multiplied by the scaling factor $\xi = 1.6 \times 10^5 \text{ G cm s}^{-1}$, chosen to bring the two curves into approximate alignment in the plot.[9,10]

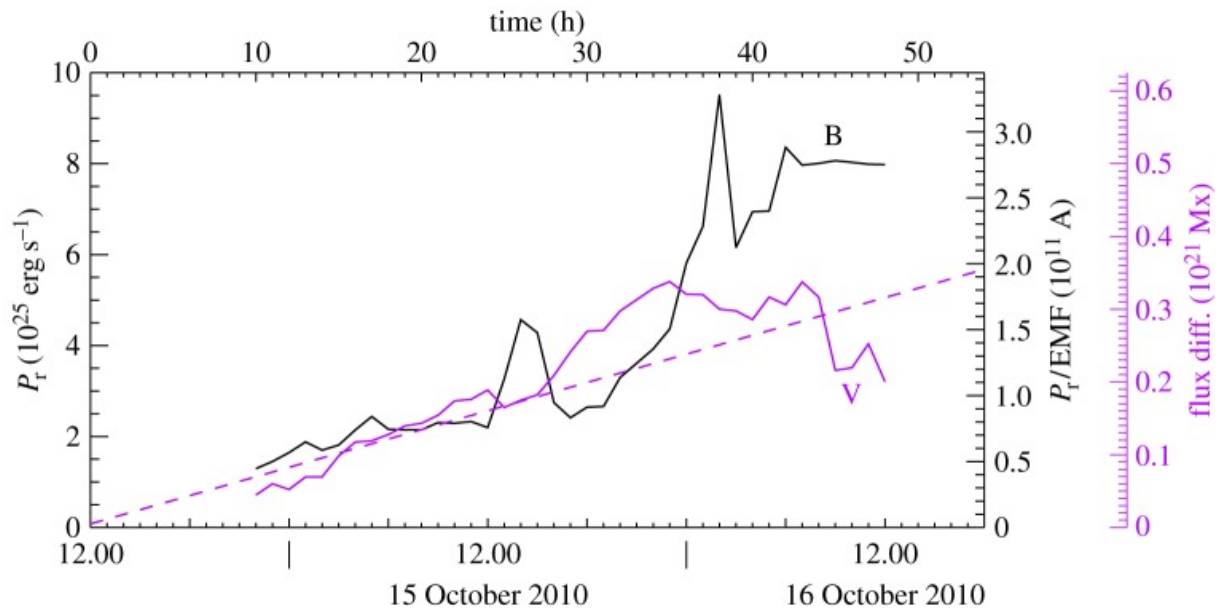


Figure 4: The radiated power P_r from the dome plasma computed from Hinode XRT filter ratios. The power is the black curve (B) read in units of $10^{25} \text{ erg s}^{-1}$ against the left axis. The same curve is scaled by $\dot{\Phi}_r \simeq 2.9 \times 10^{15}$ to yield a current, read from the inner right axis in units of 10^{11} A . The flux difference, defined by equation, is plotted in violet (V) after being scaled by the factor $\xi = 1.6 \times 10^5 \text{ G cm s}^{-1}$. It can be read from the outer right axis in units of 10^{21} Mx .

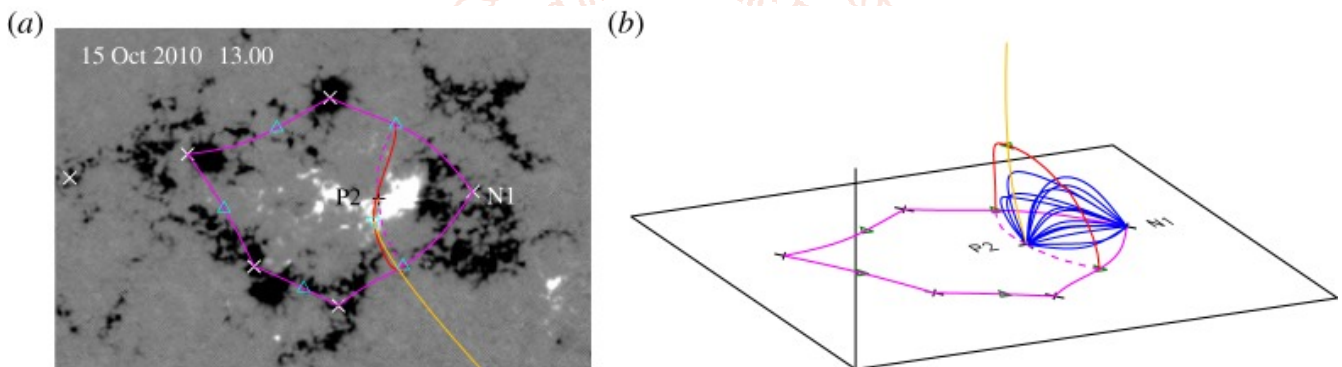


Figure 5: The MCT model of the field at 15 October 2010 13.00 (the same field as in the middle panel of figure 2). (a) The point sources, white \times s and black $+$ s, on top of the HMI radial field map (grey-scale). Photospheric negative nulls are indicated with cyan Δ and the coronal positive null with a cyan ∇ . Magenta solid curves show the spine lines from the photospheric nulls. These form a closed curve in the photosphere, which is the base of the separatrix dome—the fan surface of the coronal null. The solid orange curve shows the two spines from the coronal null (one terminates at P2 and the other connects to a positive source far away). The dashed magenta curves are the bottoms of the separatrix surfaces, which intersect the dome surface along the two separators (solid red) enclosing the P2–N1 field lines. (b) The same features in a projection, with vertical scale exaggerated for clarity. Nulls are green rather than cyan and a selection of P2–N1 interconnecting field lines are shown in blue.

The rate of observed magnetic reconnection, $\dot{\Phi} = 2.9 \times 10^{15} \text{ Mx s}^{-1}$, is equivalent to an electromotive force (EMF) of 29 MeV. If this EMF were from a simple loop, then the mean electric field, $\dot{\Phi}/L \simeq 0.6 \text{ V m}^{-1}$, would be about one hundred times greater than the Dreicer field. We do not believe that such a large electric field could actually be present. Aside from theoretical difficulties implied by such an electric field, there is absolutely no evidence of particles having energies even close to 29 MeV. This suggests to us that the electric field within the reconnecting current sheet is far more complex than a simple closed loop. The EMF might, instead, be built from numerous parallel reconnection events transferring reconnected flux through the separator loop.

Results

The average reconnection heat flux to the quiet Sun is found using the current for binary interactions. The result

$$F_H^{(QS)} \sim f v_{ph} \bar{B}^2 \quad 4.8$$

is, remarkably, independent of element size. The values quoted above yield a heat flux $F_H=10^5 \text{ erg cm}^{-2} \text{ s}^{-1}$, consistent with the heat flux inferred for quiet Sun regions

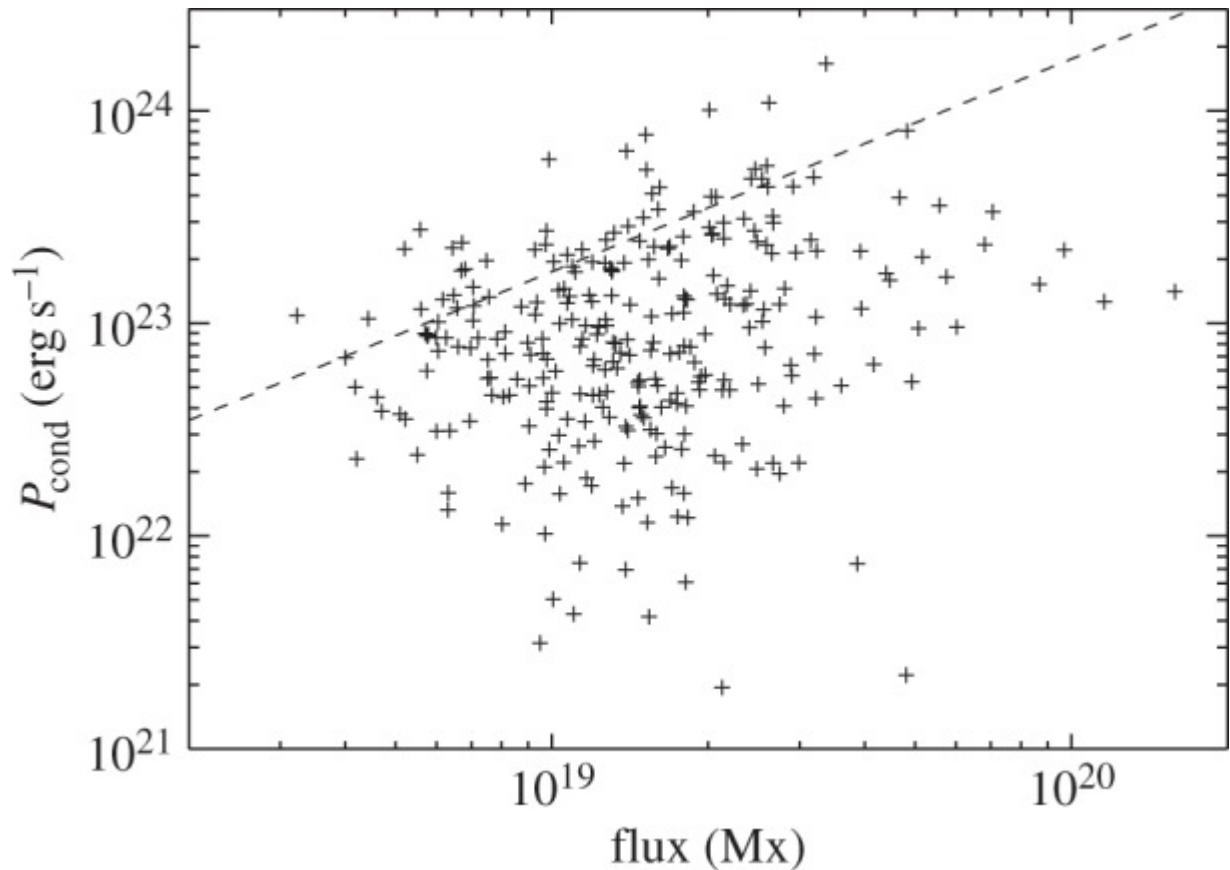


Figure 6: Power (conductive) versus flux for a survey of 285 XPSs

Unlike the quiet Sun, an active region has global currents driven on large scales. A force-free magnetic field will have a global current density $J = \alpha B$. The field is anchored to discrete elements but we will assume that current does not flow into any of the photospheric elements. Instead the coronal current will be carried along separatrices where it can close along the chromospheric canopy between concentrations. The result will be coronal current sheets confined to the peripheries of cells.[11,12] The peripheral sheet associated with a single element will carry all the current that would have otherwise entered that cell:

$$I \sim J \frac{\delta \Phi}{B} = \alpha \delta \Phi.$$

Flux transfer into or out of the domain anchored to this concentration must occur across this current sheet, thereby giving rise to electromagnetic work and heating.

$$F_H^{(AR)} \sim \alpha v_{ph} \bar{B}^{3/2} \overline{\delta \Phi}^{1/2}.$$

Conclusions

If heating power P were generated by magnetic field lines undergoing topological changes, i.e. reconnection, at a rate $\dot{\Phi}$, then the ratio of these rates, $P/\dot{\Phi}$, would have units of electric current. The

foregoing showed examples where that relation arose from an actual current in the coronal magnetic field. In those examples, the reconnection electric field does electromagnetic work on the plasma at a rate $P = I\dot{\Phi}$. This is how magnetic reconnection might heat the solar corona.[13,14]

From that basic scenario, we derived scaling laws quantifying the heat that could arise as magnetic elements move randomly over the photosphere, and coronal reconnection occurs to keep the field there from becoming excessively tangled. The process described is, at its root, the same one used by Parker to arrive at the reconnection heat flux, $F_H \sim v_{ph} B_z^2 \tan \theta$, for field lines pushed to an angle θ from their potential state

We recognize that coronal currents have different origins in ARs than in the quiet Sun: the former being globally rather than locally driven.

The weaker dependence we find on photospheric flux concentration, $F_H \sim \bar{B}^{3/2}$, may be in better agreement with observations. Some studies have synthesized EUV and X-ray images from coronal equilibrium fields with ad hoc heating fluxes $F_H \sim B^V$

Whether it supplies the majority of coronal heat or not, magnetic reconnection is clearly generating heat

in the corona at some rate. We have quantified this as the rate of electromagnetic work attributable to topological change. This is not necessarily Joule heating. In several more detailed reconnection models, this work is transferred primarily into bulk kinetic energy either in supersonic reconnection outflows, which generate heat through shocks or in magneto hydrodynamic waves, which ultimately damp to generate heat. In view of the latter option, reconnection is not necessarily an alternative to heating by waves; rather, it is a potential source of waves to heat the corona.[15]

References

- [1] Berger MA, Asgari-Targhi M. 2009. Self-organized braiding and the structure of coronal loops. *Astrophys. J.* 705, 347–355. (10.1088/0004-637X/705/1/347) [CrossRef] [Google Scholar]
- [2] Schrijver CJ, DeRosa ML, Title AM, Metcalf TR. 2005. The nonpotentiality of active-region coronae and the dynamics of the photospheric magnetic field. *Astrophys. J.* 628, 501–513. (10.1086/430733) [CrossRef] [Google Scholar]
- [3] Heyvarts J, Priest ER, Rust DM. 1977. An emerging flux model for the solar flare phenomena. *Astrophys. J.* 216, 123–137. (10.1086/155453) [CrossRef] [Google Scholar]
- [4] Longcope DW. 2001. Separator current sheets: generic features in minimum-energy magnetic fields subject to flux constraints. *Phys. Plasmas* 8, 5277–5290. (10.1063/1.1418431) [CrossRef] [Google Scholar]
- [5] Longcope DW, McKenzie D, Cirtain J, Scott J. 2005. Observations of separator reconnection to an emerging active region. *Astrophys. J.* 630, 596–614. (10.1086/432039) [CrossRef] [Google Scholar]
- [6] Tarr LA, Longcope DW, McKenzie DE, Yoshimura K. 2014. Quiescent reconnection rate between emerging active regions and preexisting field, with associated heating: NOAA AR 11112. *Solar Phys.* 289, 3331–3349. (10.1007/s11207-013-0462-x) [CrossRef] [Google Scholar]
- [7] Lemen JR, et al. 2012. The atmospheric imaging assembly (AIA) on the Solar Dynamics Observatory (SDO). *Solar Phys.* 275, 17–40. (10.1007/s11207-011-9776-8) [CrossRef] [Google Scholar]
- [8] Scherrer PH, et al. 2012. The helioseismic and magnetic imager (HMI) investigation for the Solar Dynamics Observatory (SDO). *Solar Phys.* 275, 207–227. (10.1007/s11207-011-9834-2) [CrossRef] [Google Scholar]
- [9] Tarr L, Longcope D. 2012. Calculating energy storage due to topological changes in emerging active region NOAA AR 11112. *Astrophys. J.* 749, 64 (10.1088/0004-637X/749/1/64) [CrossRef] [Google Scholar]
- [10] Longcope DW. 1996. Topology and current ribbons: model for current, reconnection and flaring in a complex, evolving corona. *Solar Phys.* 169, 91–121. (10.1007/BF00153836) [CrossRef] [Google Scholar]
- [11] Kosugi T, et al. 2007. The Hinode (Solar-B) mission: an overview. *Solar Phys.* 243, 3–17. (10.1007/s11207-007-9014-6) [CrossRef] [Google Scholar]
- [12] Narukage N, et al. 2011. Coronal-temperature-diagnostic capability of the Hinode X-ray telescope based on self-consistent calibration. *Solar Phys.* 269, 169–236. (10.1007/s11207-010-9685-2) [CrossRef] [Google Scholar]
- [13] Klimchuk JA, Cargill PJ. 2001. Spectroscopic diagnostics of nanoflare-heated loops. *Astrophys. J.* 553, 440–448. (10.1086/320666) [CrossRef] [Google Scholar]
- [14] Longcope DW, Magara T. 2004. A comparison of the minimum current corona to a magnetohydrodynamic simulation of quasi-static coronal evolution. *Astrophys. J.* 608, 1106–1123. (10.1086/420780) [CrossRef] [Google Scholar]
- [15] Longcope DW, Fisher GH. 1996. The effect of convection zone turbulence on a rising flux tube. *Astrophys. J.* 458, 380–390. (10.1086/176821) [CrossRef] [Google Scholar]